Hollow palladium–cobalt bimetallic nanospheres as an efficient and reusable catalyst for Sonogashira-type reactions

Hui Li,*[a] Zhonghong Zhu,[a] Jun Liu,[a] Songhai Xie[b] and Hexing Li*[a]

Received 15th December 2009, Accepted 11th March 2010
First published as an Advance Article on the web 26th April 2010
DOI: 10.1039/b926347k

The synthesis and characterization of hollow Pd–Co bimetallic nanospheres are reported. During Sonogashira-type coupling reactions between aryl halides and terminal alkynes in aqueous medium, these hollow materials exhibited much higher activity than the solid counterpart nanoparticles. Moreover, the catalytic activity could be adjusted *via* changing the catalyst composition. The enhanced activity was attributed to both the hollow chamber structure and the promotional effect of Co-dopants, which provided more Pd active sites for the reactants.

Introduction

The metal-catalyzed sp^2–sp coupling reaction between aryl or alkenyl halides and terminal alkynes, known as the Sonogashira reaction,[1] is one of the most important reactions for the formation of C–C bonds in organic synthesis, from both academia and industry.[2–6] Generally, homogeneous palladium salts or organometallic complexes are mainly used for the Sonogashira-type reactions.[6] However, homogeneous catalysis presents a number of drawbacks, particularly including the catalyst reusability and the environmental pollution from heavy metallic ions.[7–11] The development of heterogeneous Pd catalytic systems is a promising option to address these problems.[12–21] For nonporous Pd catalysts, very tiny Pd nanoparticles have been designed for achieving high surface area and thus activity, which, however, might inevitably cause problems in catalyst separation and reusability.[22] Meanwhile, the very tiny Pd nanoparticles also facilitate agglomeration due to high surface energy, leading to the decrease in catalytic efficiency.[23]

Hollow metal nanospheres represent a new class of powerful catalysts because of the increased surface area, low density, easy recovery, self-supporting capacity, cost reduction, and surface permeability.[24–30] Recently, we successfully synthesized Pd nanospheres with a hollow chamber using a vesicle template,[29] which exhibited much higher catalytic activity than solid Pd nanoparticles during liquid-phase phenol hydrogenation, owing to the highly dispersed Pd active sites in the unique hollow chamber. However, their industrial application is still limited due to the high cost of Pd. Obviously, design and synthesis of Pd/non-noble-metal catalysts represent a promising way to economize expensive Pd metal in the preparation of active Pd catalyst.[18,26,31]

Using polyethylene glycol spherical aggregates as a template, Bao's group successfully prepared PdCo bimetallic hollow nanospheres, which had been demonstrated to be a good catalyst for the Sonogashira reaction in aqueous media.[26] However, only PdCo catalyst with a Pd/Co atom ratio of 3.5/1 had been studied.[26] Due to the weak affinity of the oxygen atoms of polyethylene glycol for $[PdCl_4]^{2-}$, no hollow Pd nanospheres could be achieved,[26] which led to difficulty in the control of catalyst composition and thus the study of the influence of Co species on the catalytic performances. In this paper, we utilized tetrabutylphosphonium bromide (Bu_4PBr) as template. The strong electrostatic interaction between Bu_4P^+ and $[PdX_4]^{2-}$ affords $Bu_4P^+/[PdX_4]^{2-}/Co^{2+}$ composite vesicles. Such a template allows the subsequent formation of hollow Pd–Co nanospheres. Their catalytic properties are evaluated in aqueous Sonogashira-type reactions, exhibiting superior catalytic activity to the solid counterparts. More importantly, the catalytic activity of hollow Pd–Co nanospheres can be tuned by controlling their composition, which is freely adjusted through changing the molar ratio of Pd to Co in the preparation solution.

Experimental

Catalyst preparation

All of the chemicals used in this experiment were of analytical grade and used without further purification. The hollow Pd–Co catalysts were prepared according to the procedure described as follows: first, an aqueous solution of Bu_4PBr (100 mL, 0.010 M) was added into another aqueous solution composed of $PdCl_2$ (5 mL, 0.020 M) and an appropriate amount of $CoCl_2$ (0.020 M). The mixture was stirred vigorously for 2 min to form a turbid solution. Then, an appropriate amount of $NaBH_4$ aqueous solution (4.0 M) was added dropwise into the turbid solution under vigorous stirring at 303 K. After reaction was complete, the black precipitate was washed free from Cl^- or Na^+ ions with deionized water until a pH $\sim$ 7 was achieved, and finally soaked in water until the time of use. The molar ratio of B/(Pd + Co) was 4/1 to ensure the complete reduction of Pd^{2+} ions. The Co- and Pd-contents in the Pd–Co samples were adjusted by varying the molar ratio of Co^{2+}/Pd^{2+} in the precursor solution. The as-prepared Pd–Co samples in the presence of Bu_4PBr were designated Pd–Co–*x*(H) (hollow), with *x* representing the molar ratio of Co^{2+} to Pd^{2+} in the precursor solution (Table 1). For

---

[a] *Department of Chemistry and The Education Ministry Key Lab of Resource Chemistry, Shanghai Normal University, Shanghai, 200234, China. E-mail: lihui@shnu.edu.cn; hexing-li@shnu.edu.cn; Fax: +86-21-64322272; Tel: +86-21-64322642*
[b] *Department of Chemistry, Fudan University, Shanghai, 200433, China*

Table 1 Composition and catalytic properties of the as-prepared Pd–Co–x catalysts[a]

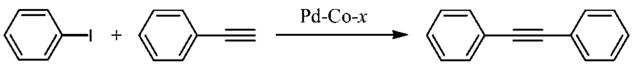

Catalyst	Nominal composition (atom%)	Bulk composition (atom%)	Conversion (%)	Selectivity (%)
Pd–Co–0(H)	Pd	Pd	54	100
Pd–Co–0.2(H)	$Pd_{83}Co_{17}$	$Pd_{84}Co_{16}$	58	100
Pd–Co–0.5(H)	$Pd_{67}Co_{33}$	$Pd_{67}Co_{33}$	74	100
Pd–Co–1(H)	$Pd_{50}Co_{50}$	$Pd_{53}Co_{47}$	99	100
Pd–Co–3(H)	$Pd_{25}Co_{75}$	$Pd_{24}Co_{76}$	87	100
Pd–Co–5(H)	$Pd_{17}Co_{83}$	$Pd_{19}Co_{81}$	85	100
Pd–Co–1(S)	$Pd_{50}Co_{50}$	$Pd_{52}Co_{48}$	68	100

[a] *Reaction conditions*: a catalyst amount containing 0.02 mmol Pd, iodobenzene (1.0 mmol), phenylacetylene (1.2 mmol), PPh_3 (0.020 mmol), CuI (0.0030 mmol), K_2CO_3 (1.5 mmol), water (3.0 mL), reaction time = 5 h, $T = 353$ K.

comparison, a solid Pd–Co catalyst was also prepared using the similar method to Pd–Co–1(H), but without adding Bu_4PBr, and was designated Pd–Co–1(S) (solid).

Catalyst characterization

The bulk composition was analyzed by means of inductively coupled plasma (ICP; Varian VISTA-MPX). The crystallinity was determined by both X-ray diffraction (XRD; Rigaku D/Max-RB with Cu-Kα radiation) and selected area electron diffraction (SAED; JEOL JEM2010). The catalyst shapes and morphologies were observed by both field emission scanning electron microscopy (FESEM; HITACHI S-4800) and transmission electron microscopy (TEM; JEOL JEM2010). The surface electronic states were investigated by X-ray photoelectron spectroscopy (XPS; ULVAC-PHI PHI5000 VersaProbe using Al-Kα radiation). All of the binding energies (BE) were calibrated by using the contaminant carbon (C 1s = 284.6 eV) as a reference. N_2 adsorption–desorption isotherms were obtained at 77 K using a Quantachrome NOVA 4000e apparatus. By N_2 adsorption, the Brunauer–Emmett–Teller (BET) surface area (S_{BET}) was calculated by using the multiple-point BET method in the relative pressure range of $P/P_0 = 0.05$–0.25.

Activity measurement

In a typical experiment, aryl halide (1.0 mmol) and phenylacetylene (1.2 mmol) were added to water (3 mL). To this were added catalyst (containing 0.02 mmol Pd), PPh_3 (0.020 mmol), CuI (0.0030 mmol) and K_2CO_3 (1.5 mmol), and the mixture was stirred at 353 K under argon. Reaction samples were taken at regular intervals and monitored by GC-MS (Agilent 6890n-5973i equipped with a DB-5 capillary column). After complete reaction, the catalyst was recovered by centrifugation and then washed thoroughly with diethyl ether. After extraction with diethyl ether, the product was analyzed by GC-MS, from which the conversion of aryl halide and the selectivity to diphenylacetylene were calculated. For the recycling test, the recovered catalyst was further washed sufficiently with ethanol and water.

Results and discussion

Structural characteristics

ICP analysis reveals that the bulk compositions in all the Pd–Co–x samples were very similar to those in the precursor solution (see Table 1).

XPS spectra (Fig. 1) show that all the Pd species in all the samples, the core level of Pd $3d_{5/2}$ was at 335.1 eV, indicating that all Pd atoms were present in the metallic state.[32] In the Co $2p_{3/2}$ level of all the Pd–Co–x samples, the peak due to metallic Co appeared at 778.0 eV.[33] In addition, the presence of $Co(OH)_2$ was confirmed by fitting the high-energy shoulders on the metallic Co line to a BE of about 781.0 eV.[33] The production of oxidized Co species could be due to the hydrolysis of BH_4^- induced by the formed metallic Pd atoms in solution, which led to the increase of the basicity of the solution and the formation of $Co(OH)_2$.[34]

The TEM image in Fig. 2a demonstrates that Pd–Co–1(S) was present in the form of solid nanoparticles. The average particle size of Pd–Co–1(S) was 8 nm. The FESEM image of Pd–Co–1(H) is shown in Fig. 2b, from which spherical particles with an average diameter around 100 nm could be clearly observed. TEM observation (Fig. 2b) further demonstrates that Pd–Co–1(H) nanospheres were hollow. Analogous morphologies and average diameter were observed for all the Pd–Co–x(H) samples. The high-magnification TEM image (Fig. 3a) reveals that the outer shell of Pd–Co–1(H) was comprised of uniform nanoparticles with an average size of 3 nm. The elemental mapping images for a single Pd–Co–1(H) sphere (Fig. 3b) show uniform distribution of Pd and Co in the hollow sphere. N_2 physisorption experiments revealed that Pd–Co–1(H) displayed type-IV adsorption/desorption isotherms with a hysteresis loop (Fig. 4), indicative of mesoporous character. This is consistent with the high-magnification TEM image (Fig. 3a), which shows wormhole-like mesopores in the outer shell. S_{BET} of Pd–Co–1(H) was determined to be 157 m^2 g^{-1}, much higher than that of Pd–Co–1(S) (44 m^2 g^{-1}), due to the formation of the hollow structure and the mesoporous

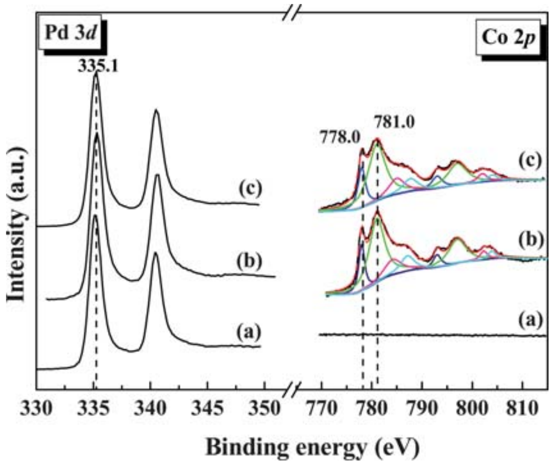

Fig. 1 XPS of (a) Pd–Co–0(H), (b) Pd–Co–1(H) and (c) Pd–Co–1(S).

shells. The high-resolution transmission electron microscopy (HRTEM) image in Fig. 5 reveals that Pd–Co–1(H) had a typical face-centered cubic (fcc) Pd structure, which corresponded to a Pd (111) interplanar spacing of 0.224 nm.

Meanwhile, the inset SAED pattern of Pd–Co–1(H) in Fig. 5 also showed diffuse rings indicative of the Pd (111), (200), (220) and (311) reflections.[35] This was consistent with the X-ray diffraction (XRD) pattern (Fig. 6), which demonstrates the fcc Pd (111), (200) and (220) diffractions (JCPDS 05-0681). The diffraction peaks for all Pd–Co–*x* were fairly broad, indicating the nanocrystalline property. Obviously, the line broadening of reflections for Pd–Co–1(H) was more intense than those for Pd–Co–1(S), which was most likely related to the decrease of particle size confirmed by TEM. The XRD pattern of the pure Co sample (Fig. 6c) prepared by reduction of Co^{2+} with $NaBH_4$ exhibited a single broad peak around $2\theta = 45°$ indicative of the amorphous structure of the Co species.[36] Due to the relatively strong signal for the Pd species, no significant diffraction peaks characteristic of Co species were detected from the XRD pattern for Pd–Co samples, which is likely related to their amorphous structure.

Our previous studies had demonstrated the synthesis of hollow Pd nanospheres is based on a vesicle-assisted chemical reduction method.[29] Likewise, the fabrication of hollow Pd–Co bimetallic nanospheres can be due to the formation of $Bu_4P^+/[PdX_4]^{2-}/Co^{2+}$ composite vesicles, which provides templates for the subsequent

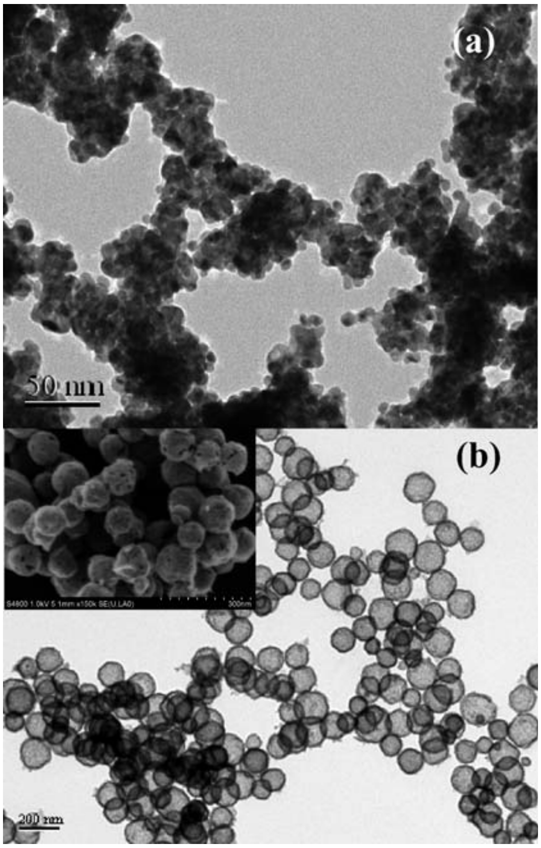

Fig. 2 TEM images of (a) Pd–Co–1(S) and (b) Pd–Co–1(H). The inset in (b) is the FESEM image of Pd–Co–1(H).

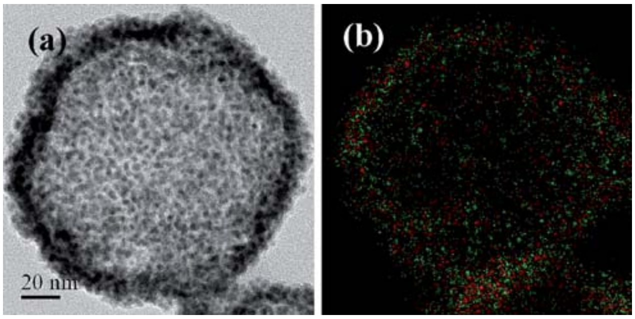

Fig. 3 (a) TEM image of a single hollow sphere in Pd–Co–1(H) and (b) elemental mapping data [Pd (red) and Co (green)] for the sphere in (a).

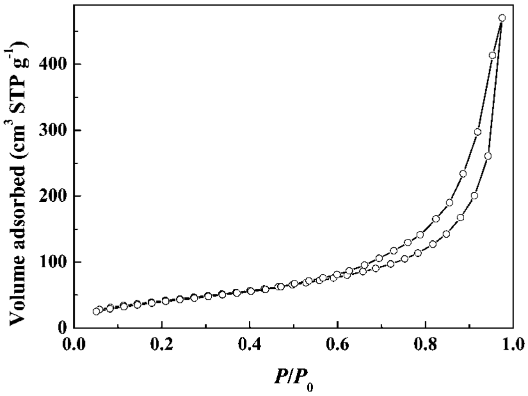

Fig. 4 N_2 adsorption/desorption isotherms of Pd–Co–1(H).

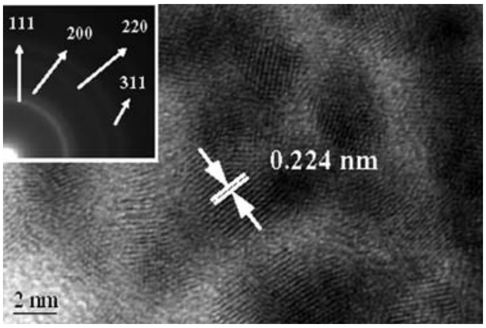

Fig. 5 HRTEM image of Pd–Co–1(H). The inset is the SAED image of Pd–Co–1(H).

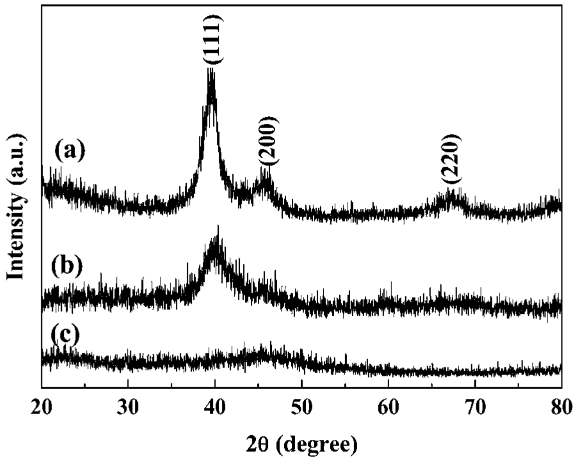

Fig. 6 XRD patterns of (a) Pd–Co–1(S), (b) Pd–Co–1(H) and (c) pure Co sample.

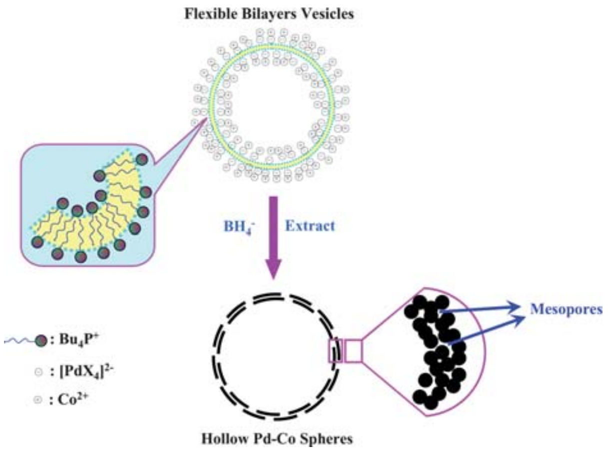

Scheme 1 The possible formation process of hollow Pd–Co nanospheres; X = Cl or Br.

growth of bimetallic shells induced by chemical reduction (see Scheme 1). Obviously, addition of $CoCl_2$ has no significant influence on the self-assembly of the hollow nanospheres.

Catalytic performances

Sonogashira-type coupling reactions between aryl halides and terminal alkynes in aqueous medium were used for evaluating the performances of the as-prepared catalyst. Fig. 7 shows the reaction profile of coupling of iodobenzene and phenylacetylene over Pd–Co–1(H), which reveals that the conversion of iodobenzene increased almost linearly with the reaction time, indicating that the present reaction was zero-order with respect to iodobenzene. A significant deviation from the straight line was observed when the iodobenzene conversion was more than 73%, possibly due to the extremely low iodobenzene concentration. The iodobenzene conversion reached 99% after reaction for 5 h. From Fig. 7, one could also see that the Pd–Co–1(H) catalyst was highly selective toward diphenylacetylene (100%). Preliminary studies also revealed that neither metallic Co nor $Co(OH)_2$ could catalyze such Sonogashira coupling reactions under the present conditions. Thus, Pd was the active sites for these reactions.

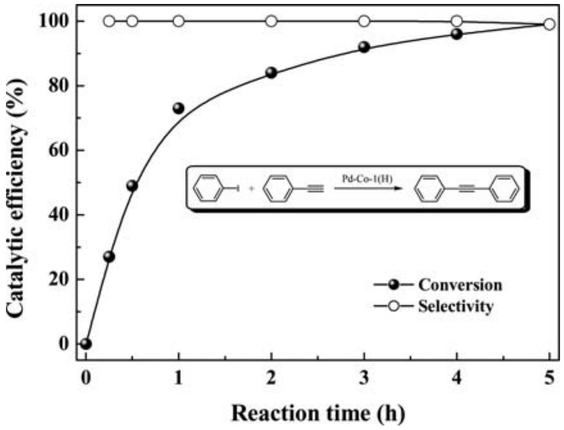

Fig. 7 Dependency of the iodobenzene conversion and the diphenylacetylene selectivity on reaction time over Pd–Co–1(H). Reaction conditions are given in Table 1.

We tested the catalytic properties of Pd–Co–*x*(H) and Pd–Co–1(S) for Sonogashira coupling reaction between iodobenzene and phenylacetylene in aqueous medium (Table 1) using the same amount of Pd in the reaction mixtures. All the Pd–Co catalysts displayed nearly 100% selectivity to diphenylacetylene. From Table 1, it could be clearly seen that the iodobenzene conversion over Pd–Co–*x*(H) first increased and then decreased with the increase of Co-content. The maximum iodobenzene conversion was obtained on Pd–Co–1(H). The promotional effect of Co-dopants on catalytic activity should be attributed to their dispersing effect on Pd active sites, which would allow more favorable oxidative addition of the metallic Pd to the carbon–halogen bond, and therefore obtain more efficient catalyst.[19] However, very high Co-content was detrimental to the activity because of the coverage of Pd active sites by the excess Co-dopants. Despite their similar composition, Pd–Co–1(H) was much more active than Pd–Co–1(S), which was also attributed to the larger number of Pd active sites, deriving from much small particle size as confirmed by TEM, XRD and S_{BET}.

Table 2 demonstrates that Pd–Co–1(H) was an active catalyst for the Sonogashira-type coupling reaction of various aryl halides and terminal alkynes. The reactants of aryl halides and terminal alkynes with electron-withdrawing or electron-donating group showed obvious difference in reactivity (entries 1–7 in Table 2), indicating that the reaction was sensitive to the electronic characteristics of the substituents under the present reaction conditions. In addition, Pd–Co–1(H) was also active for aryl bromide and even aryl chloride substrates (entries 8 and 9 in Table 2). In comparison with the PdCo bimetallic nanospheres reported by Bao's group,[26] Pd–Co–1(H) showed similarly high yield for Sonogashira coupling reactions between aryl halide and phenylacetylene in aqueous medium (entries 1 and 8 in Table 2); however, considering that the catalyst loading in our experiments was lower (2.0 mol% of Pd) than that (3.9 mol% of Pd) in Bao's work,[26] Pd–Co–1(H) obviously was more active than the catalyst prepared by Bao's method. The superior catalytic activity of Pd–Co–1(H) also can be related to the promotional effect of Co at the optimum level.

Table 2 Pd–Co–1(H) catalyzed Sonogashira coupling reactions[a]

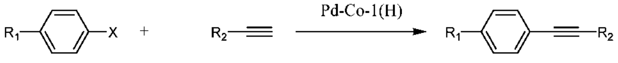

Entry	R_1	X	R_2	*t*/h	Conversion (%)	Selectivity (%)
1	H	I	Ph	5	99	100
2	Me	I	Ph	9	94	100
3	NO_2	I	Ph	4	99	100
4	OMe	I	Ph	7	95	100
5	H	I	CO_2Me	5	98	100
6	H	I	C_3H_7	7	93	100
7	H	I	CMe_2OH	7	98	100
8	H	Br	Ph	8	87	100
9[b]	H	Cl	Ph	120	70	100

[a] *Reaction conditions*: a catalyst amount containing 0.02 mmol Pd, aryl iodide (1.0 mmol), phenylacetylene (1.2 mmol), PPh_3 (0.020 mmol), CuI (0.0030 mmol), K_2CO_3 (1.5 mmol), water (3.0 mL), T = 353 K. [b] Catalyst containing 0.038 mmol Pd, T = 373 K.

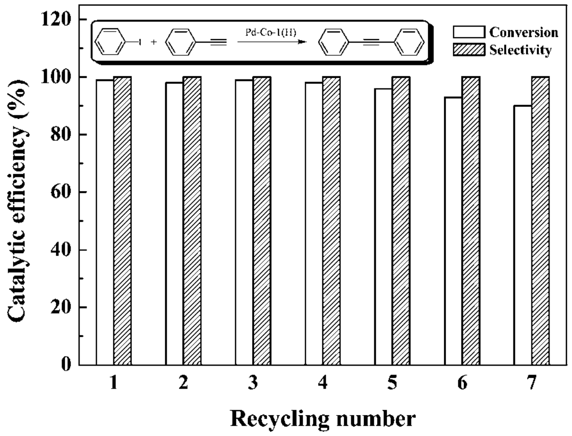

Fig. 8 Recycling test of the Pd–Co–1(H). Reaction conditions are given in Table 1.

Pd–Co–1(H) could be easily separated from the reaction solution *via* centrifugation and could be used repetitively. As shown in Fig. 8, no significant decrease in either conversion or selectivity was observed after being used seven times. This means the nature of Pd active sites did not change after being used repetitively. The catalyst weight decreased slightly after seven consecutive runs but no significant change in the composition of Pd–Co–1(H) was determined by ICP analysis. We thus consider that loss of catalyst during the separation process, rather than the leaching of Pd species from Pd–Co–1(H), was the main factor responsible for the slight decrease of the iodobenzene conversion during the recycling tests.

Conclusions

In summary, the present work reports composition controllable and easily reusable Pd–Co catalysts with hollow chamber structure prepared through a vesicle-assisted chemical reduction method. The as-prepared hollow Pd–Co catalyst exhibited much higher activity during Sonogashira-type reactions in aqueous medium relative to the solid Pd–Co nanoparticles by increasing the number of Pd active sites. Other hollow bimetallic catalysts could also be prepared based on the present method, offering more opportunities for designing new and powerful catalysts.

Acknowledgements

This work was supported by the National Natural Science Foundation of China (20973113, 20703011), the 863 Project (2007AA03Z339), the 973 Program (2009CB226106), and Shanghai Government (09JC1411400, 09YZ158, S30406, 0852nm01000).

References

1 K. Sonogashira, Y. Tohda and N. Hagihara, *Tetrahedron Lett.*, 1975, **16**, 4467.
2 K. Sonogashira, in *Comprehensive Organic Synthesis*, ed. B. M. Trost and I. Fleming, Oxford, Pergamon, 1991, vol. 3, pp. 521–549.
3 K. Sonogashira, in *Metal-Catalyzed Cross-Coupling Reactions*, ed. F. Diederich and P. J. Stang, Wiley-VCH, Weinheim, 1998, pp. 203–229.
4 K. Sonogashira, in *Handbook of Organopalladium Chemistry for Organic Synthesis*, ed. E. Negishi and A. de Meijere, Wiley-Interscience, New York, 2002, pp. 493–529.
5 K. Sonogashira, *J. Organomet. Chem.*, 2002, **653**, 46.
6 R. Chinchilla and C. Nájera, *Chem. Rev.*, 2007, **107**, 874.
7 B. Bhanage and M. Arai, *Catal. Rev. Sci. Eng.*, 2001, **43**, 315.
8 J. G. de Vries, *Can. J. Chem.*, 2001, **79**, 1086.
9 C. E. Tucker and J. G. de Vries, *Top. Catal.*, 2002, **19**, 111.
10 C. E. Garrett and K. Prasad, *Adv. Synth. Catal.*, 2004, **346**, 889.
11 C. J. Welch, J. Albaneze-Walker, W. R. Leonard, M. Biba, J. DaSilva, D. Henderson, B. Laing, D. J. Mathre, S. Spencer, X. Bu and T. Wang, *Org. Process Res. Dev.*, 2005, **9**, 198.
12 L. Yin and J. Liebscher, *Chem. Rev.*, 2007, **107**, 133.
13 M. A. De La Rosa, E. Velarde and A. Guzmán, *Synth. Commun.*, 1990, **20**, 2059.
14 K. T. Potts, C. P. Horwitz, A. Fessak, M. Keshavarz-K, K. E. Nash and P. J. Toscano, *J. Am. Chem. Soc.*, 1993, **115**, 10444.
15 M. P. López-Deber, L. Castedo and J. R. Granja, *Org. Lett.*, 2001, **3**, 2823.
16 B. M. Choudary, S. Madhi, N. S. Chowdari, M. L. Kantam and B. Sreedhar, *J. Am. Chem. Soc.*, 2002, **124**, 14127.
17 A. H. M. de Vries, J. M. C. A. Mulders, J. H. M. Mommers, H. J. W. Henderickx and J. G. de Vries, *Org. Lett.*, 2003, **5**, 3285.
18 S. U. Son, Y. Jang, J. Park, H. B. Na, H. M. Park, H. J. Yun, J. Lee and T. Hyeon, *J. Am. Chem. Soc.*, 2004, **126**, 5026.
19 C. S. Consorti, F. R. Flores and J. Dupont, *J. Am. Chem. Soc.*, 2005, **127**, 12054.
20 M. B. Thathagar, P. J Kooyman, R. Boerleider, E. Jansen, C. J. Elsevier and G. Rothenberg, *Adv. Synth. Catal.*, 2005, **347**, 1965.
21 M. B. Thathagar, J. E. ten Elshof and G. Rothenberg, *Angew. Chem., Int. Ed.*, 2006, **45**, 2886.
22 R. Schlögl and S. B. Abd Hamid, *Angew. Chem., Int. Ed.*, 2004, **43**, 1628.
23 H. Zhang, Q. Zhu, Y. Zhang, Y. Wang, L. Zhao and B. Yu, *Adv. Funct. Mater.*, 2007, **17**, 2766.
24 S. W. Kim, M. Kim, W. Y. Lee and T. Hyeon, *J. Am. Chem. Soc.*, 2002, **124**, 7642.
25 X. Chen, W. Yang, S. Wang, M. Qiao, S. Yan, K. Fan and H. He, *New J. Chem.*, 2005, **29**, 266.
26 Y. Li, P. Zhou, Z. Dai, Z. Hu, P. Sun and J. Bao, *New J. Chem.*, 2006, **30**, 832.
27 F. Cheng, H. Ma, Y. Li and J. Chen, *Inorg. Chem.*, 2007, **46**, 788.
28 P. Zhou, Y. Li, P. Sun, J. Zhou and J. Bao, *Chem. Commun.*, 2007, 1418.
29 H. Li, J. Liu, S. H. Xie, M. H. Qiao, W. L. Dai, Y. F. Lu and H. X. Li, *Adv. Funct. Mater.*, 2008, **18**, 3235.
30 H. Li, Y. Xu, J. Liu, Q. F. Zhao and H. X. Li, *J. Colloid Interface Sci.*, 2009, **334**, 176.
31 C. M. De Correa and F. C. Castrillón, *J. Mol. Catal. A: Chem.*, 2005, **228**, 267.
32 P. Weightman and P. T. Andrews, *J. Phys. C: Solid State Phys.*, 1980, **13**, L815.
33 N. S. McIntyre and M. G. Cook, *Anal. Chem.*, 1975, **47**, 2208.
34 Y. Chen, *Catal. Today*, 1998, **44**, 3.
35 M. Ganesan, R. G. Freemantle and S. O. Obare, *Chem. Mater.*, 2007, **19**, 3464.
36 H. Li, J. Liu, S. H. Xie, M. H. Qiao, W. L. Dai and H. X. Li, *J. Catal.*, 2008, **259**, 104.